

Article

Synthesis and Solution Properties of Double Hydrophilic Poly(ethylene oxide)-*block*-poly(2-ethyl-2-oxazoline) (PEO-*b*-PEtOx) Star Block Copolymers

Tobias Rudolph ^{1,2}, Sarah Crotty ^{1,2,3}, Moritz von der Luehe ^{1,2}, David Pretzel ^{1,2}, Ulrich S. Schubert ^{1,2,3} and Felix H. Schacher ^{1,2,*}

¹ Laboratory of Organic and Macromolecular Chemistry (IOMC), Friedrich Schiller University Jena, Humboldtstr. 10, Jena 07743, Germany; E-Mails: tobias.rudolph@uni-jena.de (T.R.); sarah.crotty@uni-jena.de (S.C.); moritz.von-der-luehe@uni-jena.de (M.L.); david.pretzel@uni-jena.de (D.P.); ulrich.schubert@uni-jena.de (U.S.S.)

² Jena Center for Soft Matter (JCSM), Friedrich Schiller University Jena, Philosophenweg 7, Jena 07743, Germany

³ Dutch Polymer Institute, P.O. Box 902, Eindhoven 5600 AX, The Netherlands

* Author to whom correspondence should be addressed; E-Mail: felix.schacher@uni-jena.de; Tel.: +49 (0) 3641-9-48250; Fax: +49 (0) 3641-9-48252.

Received: 28 June 2013; in revised form: 27 July 2013 / Accepted: 19 August 2013 /

Published: 2 September 2013

Abstract: We demonstrate the synthesis of star-shaped poly(ethylene oxide)-*block*-poly(2-ethyl-2-oxazoline) [PEO_m-*b*-PEtOx_n]_x block copolymers with eight arms using two different approaches, either the “arm-first” or the “core-first” strategy. Different lengths of the outer PEtOx blocks ranging from 16 to 75 repeating units were used, and the obtained materials [PEO₂₈-*b*-PEtOx_x]₈ were characterized via size exclusion chromatography (SEC), nuclear magnetic resonance spectroscopy (NMR), and Fourier-transform infrared spectroscopy (FT-IR) measurements. First investigations regarding the solution behavior in water as a non-selective solvent revealed significant differences. Whereas materials synthesized via the “core-first” method seemed to be well soluble (unimers), aggregation occurred in the case of materials synthesized by the “arm-first” method using copper-catalyzed azide-alkyne click chemistry.

Keywords: poly(2-ethyl-2-oxazoline); star-shaped block copolymers; double hydrophilic block copolymers

1. Introduction

The synthesis of polymer-based materials using different monomers, material compositions and macromolecular architectures can be realized via a multitude of synthetic methodologies. Mainly living and controlled polymerization techniques were developed to obtain polymers with narrow molar mass distributions, adjustable chain length and precisely positioned functional groups [1]. Thereby, the architecture has a large influence on the physical properties of the final material. Moreover, the monomer distribution and composition along the polymer backbone directly influences the solubility and other physical properties [2–4]. This has been demonstrated for random, gradient, graft and block copolymers synthesized by different polymerization techniques [5–9]. In the case of linear homo- and (block) copolymers, the solution behavior has become quite predictable after a manifold of systematic studies for different monomer combinations and sequences during the last few decades [10–14]. On the other hand, the combination of polymer chains in one central point leads to star-shaped materials and can result in unprecedented morphologies, as well as solution behavior in selective and non-selective solvents [15–18].

Star-shaped amphiphilic block copolymers are of special interest in drug delivery applications, due to the absence of a critical micellar concentration (cmc, depending on the hydrophilic-to-hydrophobic balance of the system) and the possibility to take up and release suitable drugs. The “load” can be encapsulated into the inner part (core, hydrophobic) of the materials, while the outer shell (hydrophilic) stabilizes the system in, e.g., aqueous solution [19]. If poly(ethylene oxide) (PEO) is used as the shell, “stealth”-behavior can be observed, also known as “PEGylation”, preventing the recognition of such materials by our immune system. This renders such approaches suitable for the preparation of long-circulating polymer-based drug nanocontainers [20–22].

For the synthesis of star-shaped block copolymers, mainly two approaches have been employed, the divergent (“core-first”) and the convergent (“arm-first”) method [20,23–27]. The divergent approach uses a multifunctional initiator, but typically not all initiation sites are easily accessible, which drastically influences the number of arms and the overall degree of polymerization. Nevertheless, with increasing distance between the core and the initiation site, the initiation efficiency can be improved. Nevertheless, star-star coupling often occurs during, e.g., radical polymerizations, and limits the monomer conversion (arm length) in such attempts [2,4,28,29]. As an alternative, the convergent approach employs pre-synthesized arms, which are subsequently connected to the core covalently in the final step, often providing superior control over arm length and number; moreover, an in-depth characterization of the constituting building blocks prior to joining the core and shell is possible. Such approaches have been described in the literature via supramolecular chemistry [24,30,31], metal-complexation [32] or click-chemistry [23,33,34].

Herein, we demonstrate the synthesis of star-shaped poly(ethylene oxide)-*block*-poly(2-ethyl-2-oxazoline) [PEO_m-*b*-PEtOx_n]_x block copolymers with eight arms using two different approaches, either the “arm-first” or the “core-first” strategy. Regarding the core block, PEO-based materials of different architectures have been thoroughly investigated concerning solution behavior [35,36] or the possibility of being scaffolds in medical applications [19,20,22]. The outer block, poly(2-ethyl-2-oxazoline) (PEtOx), is water-soluble and non-toxic, and the pseudo-peptide character of this material has been shown to induce similar “stealth” behavior, as observed for PEO [19,22,37–39]. PEtOx can be

synthesized with a wide range of functional groups, being present via cationic ring-opening polymerization (CROP) [40–43]. We used different lengths of the outer PEtOx blocks, and the obtained $[\text{PEO}_{28}\text{-}b\text{-PEtOx}_x]_8$ materials were characterized via size exclusion chromatography (SEC), nuclear magnetic resonance spectroscopy (NMR) and Fourier-transform infrared spectroscopy (FT-IR). Whereas similar compositions could be prepared using either “core-first” or “arm-first” approaches, first investigations regarding the solution behavior in water as a non-selective solvent revealed significant differences.

2. Experimental Section

2.1. Instruments

NMR: Proton nuclear magnetic resonance (^1H -NMR) spectra were recorded in CDCl_3 on a Bruker AC 300 MHz spectrometer at 298 K. Chemical shifts are given in parts per million (ppm, δ scale) relative to the residual signal of the deuterated solvent. Carbon NMR (^{13}C -NMR) spectra were recorded with 75 MHz.

SEC: Size exclusion chromatography was measured on a Shimadzu system equipped with a SCL-10A system controller, an LC-10AD pump, an RID-10A refractive index detector and both a PSS Gram30 and a PSS Gram1000 column [Polymer Standards Services GmbH (Mainz, Germany)] in series, whereby *N,N*-dimethylacetamide (DMAC) with 5 mmol of lithium chloride (LiCl) was used as an eluent at a 1 mL min^{-1} flow rate. The column oven was set to $60\text{ }^\circ\text{C}$. The system was calibrated with polystyrene (PS; 100 to $1,000,000\text{ g mol}^{-1}$) standards. Furthermore, a Shimadzu system equipped with an SCL-10A system controller, an LC-10AD pump and an RID-10A refractive index detector using a solvent mixture containing chloroform (CHCl_3), triethylamine (TEA) and *iso*-propanol (*i*-PrOH) (94:4:2) at a flow rate of 1 mL min^{-1} on a PSS SDV linear M $5\text{ }\mu\text{m}$ column. The system was calibrated using PS (100 to $100,000\text{ g mol}^{-1}$) and PEO (440 to $44,700\text{ g mol}^{-1}$) standards.

MALDI-ToF MS: Matrix-assisted laser desorption/ionization time of flight mass spectrometry was performed on an Ultraflex III TOF/TOF (Bruker Daltonics, Bremen, Germany), equipped with a Nd:YAG laser and with *trans*-2-[3-(4-*tert*-butylphenyl)-2-methyl-2-propenylidene] malononitrile (DCTB) as the matrix and NaCl as the doping agent in reflector and linear mode. The instrument was calibrated prior to each measurement with an external poly(methyl methacrylate) (PMMA) standard from PSS Polymer Standards Services GmbH (Mainz, Germany).

FT-IR Infra-red spectroscopy: Dry powders of the copolymers were directly placed on the crystal of the ATR-FTIR (Affinity-1 FTIR, Shimadzu) for measurements in the range of $4000\text{ to }600\text{ cm}^{-1}$.

Microwave-assisted polymerizations were carried out utilizing an Initiator Sixty single-mode microwave synthesizer from Biotage, equipped with a non-invasive IR sensor (accuracy: 2%). Microwave vials (conical, 0.5 to 2 mL) were heated at $110\text{ }^\circ\text{C}$ overnight and allowed to cool to room temperature under nitrogen atmosphere. All polymerizations were carried out using temperature control.

DLS: Dynamic light scattering was performed at a scattering angle of 90° on an ALV CGS-3 instrument equipped with a He-Ne laser operating at a wavelength of 633 nm at $25\text{ }^\circ\text{C}$. Tetrahydrofuran (THF) [polytetrafluoroethylene (PTFE); $0.45\text{ }\mu\text{m}$] and MilliQ-water [glass faser (GF); $1\text{--}2\text{ }\mu\text{m}$] were filtered before usage. The CONTIN algorithm was applied to analyze the obtained

correlation functions. For temperature control, the DLS is equipped with a Lauda thermostat. Apparent hydrodynamic radii were calculated according to the Stokes-Einstein equation. All CONTIN plots shown are number-weighted.

SLS: For static light scattering (SLS), different concentrations between 1.5 and 3.5 mg mL⁻¹ were prepared in THF and measured at 25 °C and different scattering angles (30° to 150°). Prior to the measurements, the samples and all solvents were filtered with PTFE-syringe filters (0.45 µm).

Liquid Chromatography under Critical Conditions (LCCC): High-performance liquid chromatography (HPLC) was measured on an Agilent system (series 1200) equipped with a binary pump, an autosampler and an evaporative light scattering detector (ELSD, Softa Corporation, Model 400). For the LCCC separation, a Nucleosil octadecylsilyl (ODS) column (Knauer, 100 mm × 3 mm, particle size 5 µm, pore size 100 Å) was used. The mobile phase consisted of a mixture of acetonitrile (ACN) and water (55/45, v/v) delivered by the binary pump at a flow rate of 0.5 mL min⁻¹. The column oven temperature was set to 45 °C. For the detection part, the ELSD was used with an evaporator temperature of 90 °C. The samples were dissolved at a concentration of 2 mg mL⁻¹ in the same solvent mixture as the mobile phase and for each measurement, 20 µL were injected. The data was acquired using the WINGPC Unity software from PSS. To characterize the star-shaped PEO samples prior to 2D measurements, size exclusion chromatography (SEC) was measured separately on a Shimadzu system equipped with an SCL-10A system controller, an LC-10AD pump and an RID-10A refractive index detector using 100% THF as the solvent at a flow rate of 3 mL min⁻¹ on a PSS-SDV-linear S column (PSS GmbH Mainz, 300 mm × 8 mm, particle size 5 µm) at 45 °C. The system was calibrated with PEO ($M_n = 1470$ to 7000 g mol⁻¹) standards purchased from PSS.

Two-dimensional liquid chromatography (2D-LC): For the first dimension LCCC of PEO, the analytical conditions were used as described above, except that the flow rate was set to 0.02 mL min⁻¹ to enable the subsequent SEC separation of the LCCC fractions for the 2D analysis. The different sample fractions of the LCCC separation were automatically transferred to the second dimension (SEC) via an eight-port valve system with 100 µL sample loops. On the SEC system, the fractions were separated on an SDV HighSpeed linear S column from PSS (50 mm × 20 mm, particle size 5 µm) using THF as eluent at a flow rate of 3 mL min⁻¹ at 45 °C and the ELSD. For the 2D measurements, higher concentrated polymer solutions (7 mg mL⁻¹) were prepared, and 50 µL were used as the injection volume. The data acquisition was done by the PSS WINGPC unity software, including a 2D software module.

Transmission electron microscopy (TEM): The formed aggregates were analyzed using a TEM (Zeiss-CEM 902A, Oberkochen, Germany) operated at 80 kV. Images were recorded using a 1 k TVIPS FastScan CCD camera. TEM samples were prepared by applying a drop of an aqueous sample solution onto the surface of a plasma-treated carbon coated copper grid (Holey Carbon Grid + 2 nm C; Quantifoil Micro-Tools GmbH, Jena, Germany).

2.2. Materials

Star-shaped poly(ethylene oxide) ([PEO-OH]₈; supplier information: $M_n = 10,000$ g mol⁻¹; SEC (CHCl₃/*i*-PrOH/Et₃N): $M_n = 6100$ g mol⁻¹, Đ 1.07; SEC (DMAC/LiCl): $M_n = 6800$ g mol⁻¹; Đ = 1.11; MALDI-ToF MS: $M_p = 9900$ g mol⁻¹) (JenKem Technology, China) was dissolved in THF and

precipitated in cold diethyl ether, filtered and dried under vacuum before usage. Tetrahydrofuran (THF), acetonitrile (ACN) and dichloromethane (DCM) were purified using a Solvent Purification System (SPS, Innovative Technology, PM-400-3-MD) equipped with two activated alumina columns. 2-Ethyl-2-oxazoline (EtOx) and propargyl *p*-toluenesulfonate (Aldrich) were distilled over barium oxide under reduced pressure before polymerization and stored under argon. Triethylamine was distilled over CaH₂ and stored under argon. All other chemicals were used as purchased if not otherwise mentioned in the text.

2.2.1. Tosylation of Star-Shaped [PEO₂₈-OH]₈

The tosylation of [PEO₂₈-OH]₈ (6 g; 0.6 mmol) was achieved in a slightly modified way as described in the literature [44,45]. Briefly, the educts were dissolved in DCM and stirred at room temperature for at least 72 h, obtaining [PEO₂₈-Ts]₈ via extraction and precipitation in cold diethyl ether.

SEC (CHCl₃/*i*-PrOH/Et₃N): $M_n = 6300 \text{ g mol}^{-1}$; $\bar{D} = 1.10$ (PEO-calibration); SEC (DMAC/LiCl): $M_n = 5800 \text{ g mol}^{-1}$; $\bar{D} = 1.22$ (PEO-calibration); ¹H NMR (300 MHz, CDCl₃, δ): 7.84–7.14 (aromatic CH), 4.15 (t, Ts-CH₂-CH₂-O-), 3.80–3.46 (b, -CH₂-CH₂-O-), 2.44 (s, methyl) ppm; ¹³C-NMR (75 MHz, CDCl₃, δ): 125–130 (aromatic CH), 71–70 (backbone), ppm 69.1 (-CH₂-CH₂-Ts), 68.5 (-CH₂-CH₂-Ts), 21.2 (Ts-CH₃) ppm.

2.2.2. Preparation of Star-Shaped [PEO₂₈-N₃]₈

[PEO₂₈-Ts]₈ (4 g; 0.4 mmol) was dissolved in DMF (10 mL) and stirred together with sodium azide (NaN₃, 20 equiv) overnight at room temperature. The solvent was removed under reduced pressure and the remainder diluted with chloroform and extracted with water, filtered and dried over sodium sulfate. The resulting [PEO₂₈-N₃]₈ was obtained as a brownish powder via precipitation in cold diethyl ether.

SEC (CHCl₃/*i*-PrOH/Et₃N): $M_n = 7000 \text{ g mol}^{-1}$; $\bar{D} = 1.10$ (PEO-calibration); SEC (DMAC/LiCl): $M_n = 5800 \text{ g mol}^{-1}$; $\bar{D} = 1.21$ (PEO-calibration); ¹H NMR (300 MHz, CDCl₃, δ): 3.80–3.46 (b, -CH₂-CH₂-O-) ppm; ¹³C-NMR (75 MHz, CDCl₃, δ): 71–70 (backbone), ppm 69.8 (-CH₂-CH₂-N₃), 50.5 (-CH₂-CH₂-N₃) ppm; ATR-FT-IR: 2110 cm⁻¹ (azide).

2.2.3. Synthesis of Alkyne-Functionalized TB-PEtOx_x

Propargyl *p*-toluenesulfonate and 2-ethyl-2-oxazoline (EtOx) were dissolved in acetonitrile (ACN) at different monomer to initiator ratios ([M]/[I] = 20, 60 and 80) at a monomer concentration of 4 M. The capped vials were placed in a microwave synthesizer at 140 °C. The polymerization was terminated via the addition of water. The polymers were obtained after extraction with NaHCO₃ solution, brine and dried under vacuum. After precipitation in cold diethyl ether, the polymer was filtered and dried under vacuum.

TB-PEtOx₁₈: SEC (CHCl₃/*i*-PrOH/Et₃N): $M_n = 2700 \text{ g mol}^{-1}$; $\bar{D} = 1.12$ (PS-calibration); SEC (DMAC/LiCl): $M_n = 3900 \text{ g mol}^{-1}$; $\bar{D} = 1.18$ (PS-calibration); TB-PEtOx₅₅: SEC (CHCl₃/*i*-PrOH/Et₃N): $M_n = 5600 \text{ g mol}^{-1}$; $\bar{D} = 1.09$ (PS-calibration); SEC (DMAC/LiCl): $M_n = 9700 \text{ g mol}^{-1}$; $\bar{D} = 1.16$ (PS-calibration); TB-PEtOx₇₅: SEC (CHCl₃/*i*-PrOH/Et₃N): $M_n = 7000 \text{ g mol}^{-1}$; $\bar{D} = 1.10$ (PS-calibration); SEC (DMAC/LiCl): $M_n = 12,000 \text{ g mol}^{-1}$; $\bar{D} = 1.19$ (PS-calibration); ¹H NMR

(300 MHz, CDCl_3 , δ): 3.6–3.2 (br, $-\text{N}-\text{CH}_2-\text{CH}_2-$), 2.5–2.2 (br, $\text{CO}-\text{CH}_2-\text{CH}_3$), 1.2–0.9 (br, $\text{CO}-\text{CH}_2-\text{CH}_3$).

2.2.4. Copper catalyzed Azide-Alkyne Cycloaddition (CuAAC) Click Reaction between $[\text{PEO}_{28}\text{-N}_3]_8$ and TB-PEtOx_x

For the microwave-assisted copper-catalyzed azide-alkyne cycloaddition click chemistry (CuAAC) click reaction $[\text{PEO}_{28}\text{-N}_3]_8$ (1 equiv) and TB-PEtOx_x (16 equiv) were dissolved in a solvent mixture of ethanol (EtOH) and THF (1:1 vol %). Copper bromide (CuBr; 10 equiv) and *N,N,N',N'',N'''*-Pentamethyldiethylenetriamine (PMDETA; 10 equiv) were added under argon flux, purged for 15 min with argon and placed in the microwave-synthesizer for 30 min at 80 °C. The solvent was removed under reduced pressure, and the copper was removed via a short aluminum oxide (AlOxN) column. The homopolymer was removed via precipitation in THF at −30 °C.

$[\text{PEO}_{28}\text{-}b\text{-PEtOx}_{18}]_8$: SEC (DMAC/LiCl): $M_n = 22,000 \text{ g mol}^{-1}$; $\bar{D} = 1.13$ (PS-calibration); $[\text{PEO}_{28}\text{-}b\text{-PEtOx}_{55}]_8$: SEC (DMAC/LiCl): $M_n = 46,000 \text{ g mol}^{-1}$; $\bar{D} = 1.18$ (PS-calibration); $[\text{PEO}_{28}\text{-}b\text{-PEtOx}_{75}]_8$: SEC (DMAC/LiCl): $M_n = 42,000 \text{ g mol}^{-1}$; $\bar{D} = 1.14$ (PS-calibration); ^1H NMR (300 MHz, CDCl_3 , δ): 4.0–3.0 (br, backbone), 2.6–2.2 (br, $\text{CO}-\text{CH}_2-\text{CH}_3$), 1.2–0.8 (br, $\text{CO}-\text{CH}_2-\text{CH}_3$).

2.2.5. Polymerization of 2-Ethyl-2-oxazoline using a Star-Shaped PEO Macroinitiator

For the polymerization of EtOx via a star-shaped macroinitiator $[\text{PEO}_{28}\text{-Ts}]_8$, different initiator to monomer ratios were chosen, and the polymerization was conducted in acetonitrile (1 M) in a microwave-synthesizer at 140 °C. The reaction was stopped via cooling the reaction mixture after 15 min and the addition of 0.2 mL of water. The final polymer was obtained via precipitation in THF at −30 °C.

$[\text{PEO}_{28}\text{-}b\text{-PEtOx}_{16}]_8$: SEC (DMAC/LiCl): $M_n = 24,000 \text{ g mol}^{-1}$; $\bar{D} = 1.24$ (PS-calibration); $[\text{PEO}_{28}\text{-}b\text{-PEtOx}_{50}]_8$: SEC (DMAC/LiCl): $M_n = 35,000 \text{ g mol}^{-1}$; $\bar{D} = 1.15$ (PS-calibration); ^1H NMR (300 MHz, CDCl_3 , δ): 4.0–3.0 (br, backbone), 2.6–2.2 (br, $\text{CO}-\text{CH}_2-\text{CH}_3$), 1.2–0.8 (br, $\text{CO}-\text{CH}_2-\text{CH}_3$).

2.2.6. Kinetic Investigation of the Polymerization of 2-Ethyl-2-oxazoline using a Star-Shaped PEO-Macroinitiator

A stock solution of the macroinitiator $[\text{PEO}_{28}\text{-Ts}]_8$ and 2-ethyl-2-oxazoline (EtOx) were mixed with acetonitrile at a monomer to initiator ratio of 40 and a monomer concentration of 1 M. The capped vials were placed in a microwave synthesizer at 140 °C. The polymerization was terminated via the addition of water. The pure star-shaped block copolymers were received after precipitation in THF at −30 °C.

3. Results and Discussion

We were interested in the solution properties of well-defined star-shaped block copolymers containing two hydrophilic blocks. In particular, the influence of the length used for the outer block on the behavior in non-selective solvents (*i.e.*, water) for a system with a given arm number (here: eight

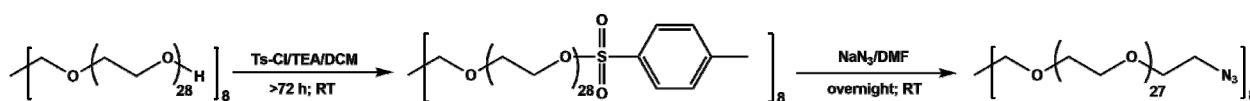
arms) was our focus for this study. We chose poly(ethylene oxide) as the core, due to its wide solubility in common solvents, its commercial availability and chemical inertness, enabling various chemical modifications. As the outer block (shell), we used poly(2-ethyl-2-oxazoline), a well-studied material with proven biocompatibility [22] and temperature-responsive properties (lower critical solution properties, LCST) above a threshold-molar mass in aqueous media [46,47].

Regarding the synthesis of star-shaped poly(ethylene oxide)-*block*-poly(2-ethyl-2-oxazoline) block copolymers with eight arms, we chose to compare two different strategies: for the “arm-first” approach, the macromolecular conjugation (azide-alkyne click reaction [27,48]) between azide-functionalized $[\text{PEO}_{28}\text{-N}_3]_8$ and alkyne-functionalized TB-PEtOx_x of different molar mass was used. In the case of the “core-first” strategy, tosylated $[\text{PEO}_{28}\text{-Ts}]_8$ (the subscripts denote the degree of polymerization of the corresponding block, and the subscripts after the brackets represent the arm number of the herein described star-shaped block copolymers) was used as a macroinitiator for the cationic ring-opening polymerization (CROP) of 2-ethyl-2-oxazoline (EtOx). In both cases, the length of the PEtOx block can be easily varied within a certain range. In the following, first, both synthetic routes will be described separately, and afterwards, the solution properties in water as a non-selective solvent for both blocks will be compared.

3.1. Star Synthesis via Macromolecular Conjugation (“Arm-First”-Approach)

Core: First, a commercially available star-shaped poly(ethylene oxide) (PEO) with eight arms and a total molar mass (M_n) of $10,000 \text{ g mol}^{-1}$ (1250 g mol^{-1} per arm) was modified. For this purpose, the hydroxyl end group was tosylated first by a nucleophilic substitution reaction using *p*-toluenesulfonyl chloride (Ts-Cl; Scheme 1), obtaining $[\text{PEO-Ts}]_8$. Whereas this modification for linear PEO is often described as being performed within a few hours [44,45], in our case, the reaction time needed to be increased to at least 72 h at room temperature to achieve full functionalization (determined via $^1\text{H-NMR}$; Figure S1C).

Scheme 1. Preparation of $[\text{PEO}_{28}\text{-Ts}]_8$ and $[\text{PEO}_{28}\text{-N}_3]_8$.

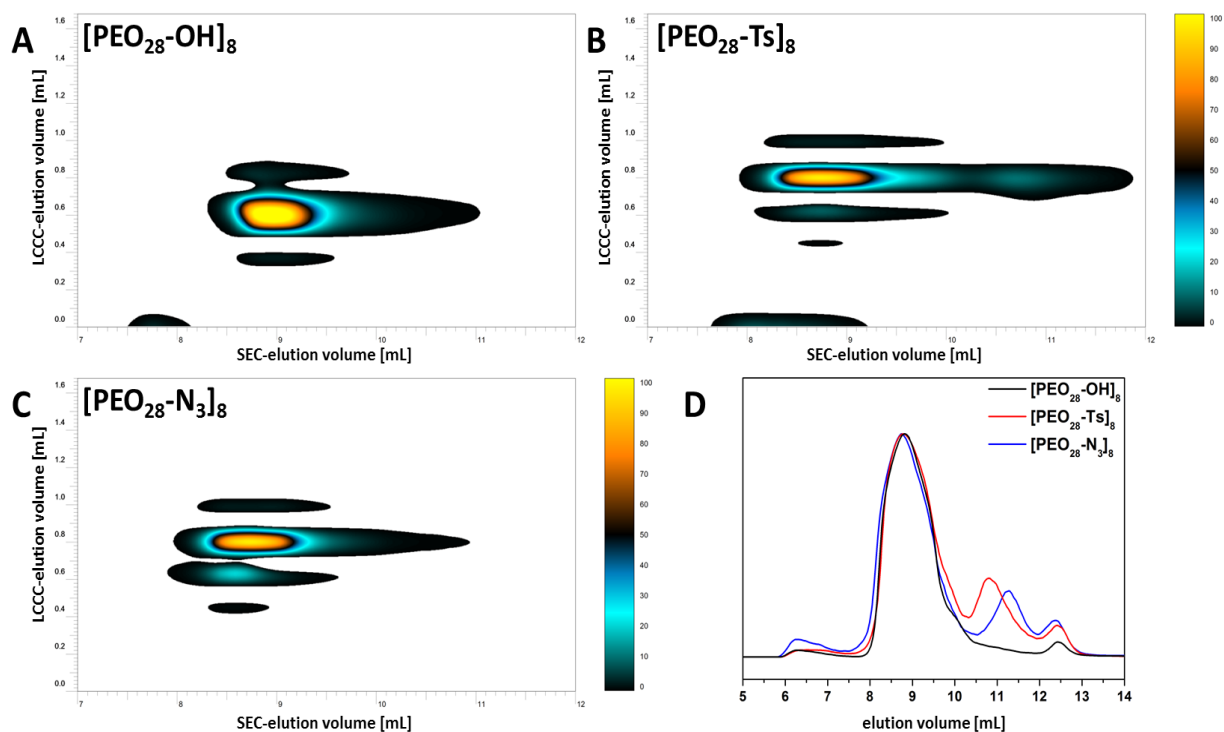


Afterwards, $[\text{PEO}_{28}\text{-Ts}]_8$ was converted to $[\text{PEO}_{28}\text{-N}_3]_8$ using sodium azide (Scheme 1). After purification, for $[\text{PEO}_{28}\text{-N}_3]_8$, slight amounts (<5%) of residual aromatic signals, corresponding to the tosyl-moiety, were observed via $^1\text{H NMR}$ (Figure S1C). Nevertheless, the azide group could be clearly detected by ATR FT-IR measurements (2110 cm^{-1} ; Figure S1B).

To ensure full end-group conversion of the modified star-shaped macromolecules, the polymers were investigated via $^{13}\text{C-NMR}$ and 2D-LC (LCCC \times SEC). In the latter case, liquid chromatography under critical conditions for PEO (LCCC) should enable the separation according to the end-group polarity and further coupled to SEC for the molar range [49–53]. After careful adjustment of the critical conditions for PEO (Figure S2), the stars with different end-groups ($[\text{PEO}_{28}\text{-OH}]_8$, $[\text{PEO}_{28}\text{-Ts}]_8$ and $[\text{PEO}_{28}\text{-N}_3]_8$) were investigated (Figure 1). As can be seen, $[\text{PEO}_{28}\text{-OH}]_8$ exhibits only one distribution, with a peak maximum at 0.62 mL (Figure 1A), whereas for $[\text{PEO}_{28}\text{-Ts}]_8$, two distributions

at 0.80 mL (97%) and 0.62 mL (3%, unfunctionalized material) were observed (Figure 1B). This is in good agreement with the error of the NMR spectroscopy, where no $[\text{PEO}_{28}\text{-OH}]_8$ could be detected. For $[\text{PEO}_{28}\text{-N}_3]_8$, also, two distributions at 0.80 mL (90%) and at 0.62 mL (10%) were observed (Figure 1C). We tentatively attribute this observation to a slow exchange of the azide functionality by hydroxyl groups under these conditions. This assumption can be confirmed by time-dependent investigations, leading to a ratio of 90:10 for both distributions directly after sample preparation, while 75:25 is found after 30 min (Figure S3). If the sample was stored overnight in solution, a ratio of 50:50 is observed. As many reactions using azides are described in the literature in water [49,54], this exchange process might be facilitated here, as the sample is heated to 45 °C and remains for 100 min within the system to elute/separate.

Figure 1. 2D-LC results (acetonitrile (ACN)/H₂O 55/45 v/v) for $[\text{PEO}_{28}\text{-OH}]_8$ (A), $[\text{PEO}_{28}\text{-Ts}]_8$ (B) and $[\text{PEO}_{28}\text{-N}_3]_8$ (C); in comparison with the SEC traces obtained for $[\text{PEO}_{28}\text{-OH}]_8$ (solid black line), $[\text{PEO}_{28}\text{-Ts}]_8$ (solid red line) and $[\text{PEO}_{28}\text{-N}_3]_8$ (solid blue line; THF was used as eluent).



The elution behavior in LCCC was similar for $[\text{PEO}_{28}\text{-Ts}]_8$ and $[\text{PEO}_{28}\text{-N}_3]_8$, again, somewhat surprising. During SEC, further small distributions appear at higher elution volumes, which might be due to a higher flow rate of 3 mL min⁻¹ (Figure 1D), as under flow rates of 1 mL min⁻¹, only monomodal distributions were observed.

Due to the results obtained for $[\text{PEO}_{28}\text{-N}_3]_8$ using 2D-LC experiments, additional ¹³C-NMR measurements in CDCl₃ were carried out. Here, the signals for the tosyl-group, as well as the CH₂-group located next to the hydroxyl-end-group at 61.5 ppm are not observed, and also, two new signals for the two CH₂ groups next to the azide functionality at 50.5 and 79.8 ppm (Figure S4) confirm the successful conversion, at least within the experimental error of the NMR [45,55].

Arm: Alkyne-functionalized 2-ethyl-2-oxazoline homopolymers (TB-PEtOx_x) with different molar masses and low polydispersity indices (\bar{D} ; <1.1) were obtained via microwave-assisted cationic ring-opening polymerization (CROP) of 2-ethyl-2-oxazoline (EtOx) [25]. Therefore, solutions containing a functional initiator, propargyl *p*-toluenesulfonate, with different monomer-to-initiator ratios ($[M]/[I]$) at a constant monomer concentration of 4 M were prepared and polymerized in a microwave-synthesizer at 140 °C. The degrees of polymerization (DP) obtained via ¹H NMR and MALDI-ToF MS slightly differ from the theoretically calculated values, according to the feed ratios used for the polymerizations. For a theoretical DP of 20, a DP of 18 (TB-PEtOx₁₈), for a DP of 60, a DP of 55 (TB-PEtOx₅₅), and for a DP of 80, a DP of 75 (TB-PEtOx₇₅) were found (Table 1, SEC in Figure S6A).

Table 1. Selected characterization data for alkyne-functionalized poly(2-ethyl-2-oxazoline)s (TB-PEtOx_x) and star-shaped [PEO₂₈-Y]₈.

Sample	DP ^a	M _n ^b [g mol ⁻¹]	M _n ^c [g mol ⁻¹]	\bar{D} ^c	M _p ^d [g mol ⁻¹]	Building Block
TB-PEtOx ₁₈ ^{b,e}	20	1800	2700	1.12	1500	arm in chloroform
TB-PEtOx ₅₅ ^{b,e}	60	5500	5600	1.09	5400	
TB-PEtOx ₇₅ ^{b,e}	80	7500	6700	1.10	7200	
TB-PEtOx ₁₈ ^{e,f}	20	1800	3900	1.18	—	arm in DMAC
TB-PEtOx ₅₅ ^{e,e}	60	5500	9700	1.16	—	
TB-PEtOx ₇₅ ^{e,e}	80	7500	12,000	1.19	—	
[PEO ₂₈ -OH] ₈ ^{b,e}	—	10,000	6100 ^h	1.07	9,900	star-shaped core
[PEO ₂₈ -Ts] ₈ ^{b,e}	—	11,000	7000 ^h	1.04	—	
[PEO ₂₈ -N ₃] ₈ ^{b,e}	—	10,300	7000 ^h	1.07	—	
[PEO ₂₈ -N ₃] ₈ ^{e,g}	—	10,300	12,000 ^g	1.15	—	

^a feed ratio $[M]/[I]$; ^b calculated from nuclear magnetic resonance spectroscopy (NMR) and Matrix-assisted laser desorption/ionization time of flight mass spectrometry (MALDI-ToF MS); ^c size exclusion chromatography (SEC) (CHCl₃/*i*-PrOH/TEA) (PS-calibration); ^d MALDI-ToF MS (matrix/doping agent *trans*-2-[3-(4-*tert*-butylphenyl)-2-methyl-2-propenylidene] malononitrile (DCTB) /NaCl); ^e subscripts denote the degree of polymerization; ^f SEC (DMAC/LiCl) (PS-calib.); ^g SEC (DMAC/LiCl) (PEO-calib.); ^h SEC (CHCl₃/*i*-PrOH/TEA) (PEO-calib.).

The molar masses of the polymers increase linearly with the monomer-to-initiator ratio and are also in good agreement with the values obtained by MALDI-ToF MS measurements (Table 1). As the molar masses of the star-shaped block copolymers after arm attachment will exceed the exclusion volume of the utilized CHCl₃ SEC, the homopolymers (arms) were also subjected to another SEC instrument featuring a higher molar mass range (here, *N,N*-dimethylacetamide (DMAc) was used as the eluent, Figure S6B). The slight broadening of the \bar{D} -values can be ascribed to polymer-column interactions, and, furthermore, the apparent molar masses are higher in comparison to the values obtained using chloroform as the eluent.

For the synthesis of [PEO₂₈-*b*-PEtOx_x]₈, star-shaped block copolymers [PEO₂₈-N₃]₈ and different TB-PEtOx_x were used in copper-catalyzed azide-alkyne cycloaddition reactions (CuAAC; Scheme 2). First, the conditions had to be optimized by variation of the solvent, the reaction temperature and the reaction time. The best conditions were obtained in a THF-ethanol mixture (1:1 v/v) at 80 °C using a four-fold excess of TB-PEtOx_x in comparison to the azide-functionality and a reaction time of only 15 min in the microwave synthesizer. Under these conditions, it was possible to obtain the desired

[PEO₂₈-*b*-PEtOx_x]₈ materials. Purification was achieved via selective precipitation of the block copolymer in THF at −30 °C, while PEtOx_x homopolymers are still soluble under these conditions. The obtained polymers were characterized using SEC (Table 2), FT-IR and NMR (Figure S7).

Scheme 2. Schematic representation of the synthesis of star-shaped [PEO₂₈-*b*-PEtOx_x]₈ block copolymers using copper-catalyzed azide-alkyne cycloaddition click chemistry (CuAAC).

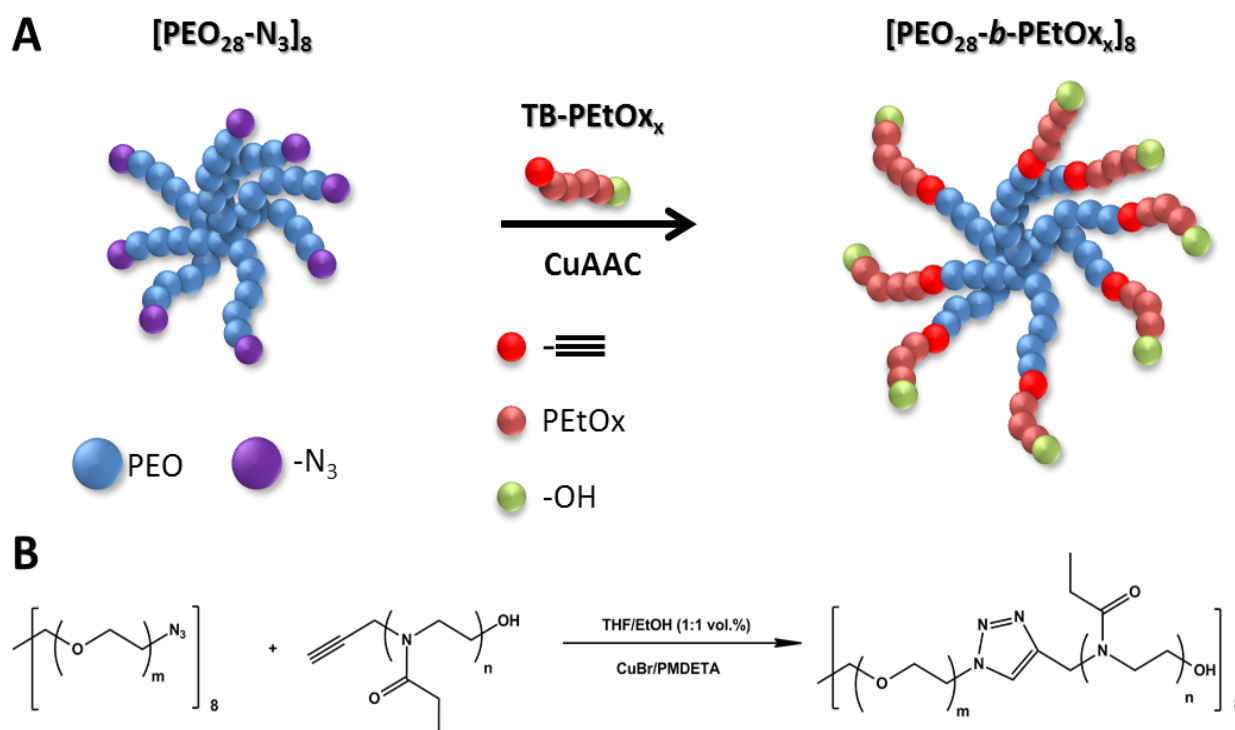


Table 2. Selected characterization data for star-shaped [PEO₂₈-*b*-PEtOx_x]₈ block copolymers obtained via the “core-first” or “arm-first” approach.

Sample	M_n^a [g mol ^{−1}]	\bar{D}^a	$M_{n,calc}^b$ [g mol ^{−1}]	$M_{w,SLS}^d$ [g mol ^{−1}]	Approach
[PEO ₂₈ - <i>b</i> -PEtOx ₁₈] ₈ ^c	22,000	1.13	22,000	—	arm-first
[PEO ₂₈ - <i>b</i> -PEtOx ₅₅] ₈ ^c	46,000	1.18	54,000	—	
[PEO ₂₈ - <i>b</i> -PEtOx ₇₅] ₈ ^c	42,000	1.14	67,000	—	
[PEO ₂₈ - <i>b</i> -PEtOx ₁₆] ₈ ^c	24,000	1.24	22,000	—	core-first
[PEO ₂₈ - <i>b</i> -PEtOx ₅₀] ₈ ^c	35,000	1.15	50,000	54,000	

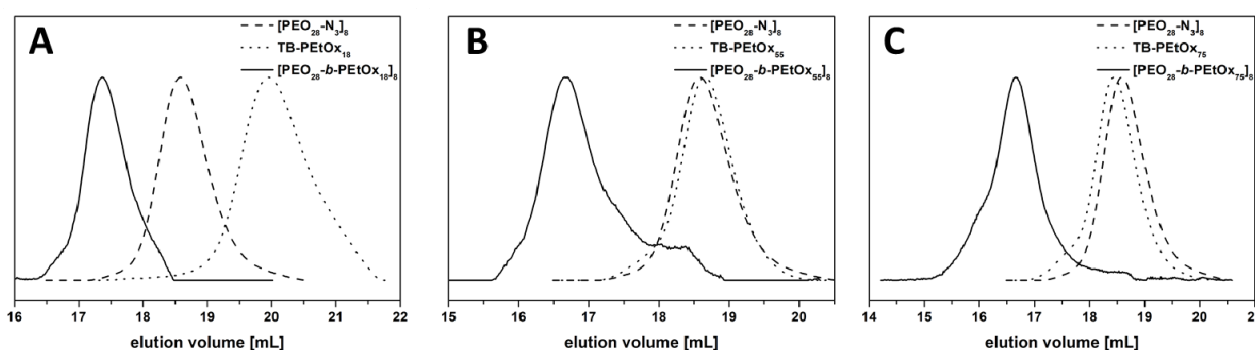
^a SEC (DMAC/LiCl) (PS-calib.); ^b calculated from the single compound molar masses obtained via MALDI-ToF MS (“arm-first”) or ¹H-NMR (“core-first”); ^c subscripts denote the number of repeating units;

^d static light scattering at 25 °C in THF ($dn/dc = 0.0915$ mL g^{−1}; $A_2 = 1 \times 10^{-8}$ mol dm³ g^{−2}).

SEC elution traces using DMAC/LiCl (0.21 wt % LiCl) as the eluent for the individual building blocks and the star-shaped block copolymers are shown in Figure 2. The corresponding characterization data are shown in Table 2. Via this approach, three different star-shaped block copolymers, [PEO₂₈-*b*-PEtOx₁₈]₈, [PEO₂₈-*b*-PEtOx₅₅]₈ and [PEO₂₈-*b*-PEtOx₇₅]₈, were obtained. Owing to the star architecture, the elution behavior of the star-shaped block copolymers leads to lower molar masses than expected during SEC measurements. This effect has already been described for other

star-shaped and branched systems [3]. According to the SEC traces, e.g., in the case of $[\text{PEO}_{28}\text{-}b\text{-PEtOx}_{18}]_8$, a clear shift for $[\text{PEO}_{28}\text{-}b\text{-PEtOx}_{18}]_8$, if compared to TB-PEtOx₁₈ and $[\text{PEO}_{28}\text{-N}_3]_8$, can be observed. Moreover, after purification, the sample contained neither an excess of the arm (TB-PEtOx₁₈) nor the core $[\text{PEO}_{28}\text{-N}_3]_8$. The apparent molar masses of $[\text{PEO}_{28}\text{-}b\text{-PEtOx}_{18}]_8$ obtained by SEC are $22,000\text{ g mol}^{-1}$ with a narrow Đ-value of 1.13 (PS-calibration). The apparent molar masses for $[\text{PEO}_{28}\text{-}b\text{-PEtOx}_{55}]_8$ and $[\text{PEO}_{28}\text{-}b\text{-PEtOx}_{75}]_8$ are in a comparable range with 46,000 and 42,000 g mol^{-1} . The composition of the star-shaped block copolymers was further confirmed using $^1\text{H-NMR}$ (Figure S7B).

Figure 2. SEC traces using DMAC/LiCl as the eluent for TB-PEtOx_x (dotted line), $[\text{PEO}_{28}\text{-N}_3]_8$ (scattered line) and the obtained purified star-shaped $[\text{PEO}_{28}\text{-}b\text{-PEtOx}_x]_8$ (solid line): (A) $[\text{PEO}_{28}\text{-}b\text{-PEtOx}_{18}]_8$; (B) $[\text{PEO}_{28}\text{-}b\text{-PEtOx}_{55}]_8$; (C) $[\text{PEO}_{28}\text{-}b\text{-PEtOx}_{75}]_8$.

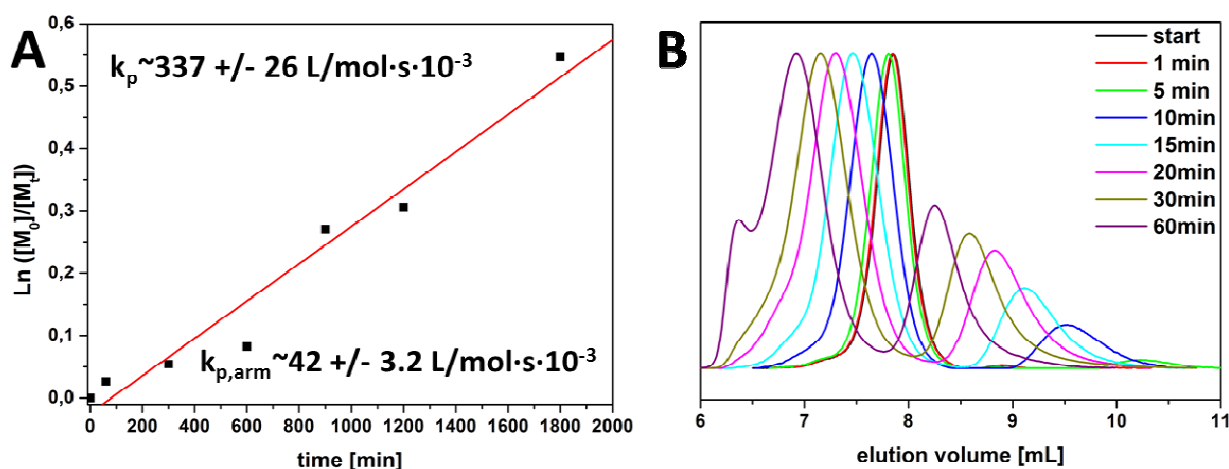


3.2. Star Synthesis via CROP of 2-Ethyl-2-oxazoline Using a Star-Shaped Macroinitiator (“Core-First”-Approach)

Furthermore, here, commercially available $[\text{PEO}_{28}\text{-OH}]_8$ was modified via tosylation as described above and purified until no further unreacted Ts-Cl could be observed in the $^1\text{H-NMR}$ spectra. As PEO is rather hydroscopic, the macroinitiator was co-evaporated with toluene, dried under vacuum for at least 24 h and stored in a glove box. After the preparation of the macroinitiator, we first carried out a kinetic study for the polymerization of EtOx (Figure 3). Therefore, a stock solution of $[\text{PEO}_{28}\text{-Ts}]_8$ and monomer ($[\text{M}]/[\text{I}] = 40$) was prepared in ACN (1M) and divided into several microwave vials. The vials were subsequently placed in the microwave-synthesizer and analyzed after different polymerization times at 140 °C via $^1\text{H-NMR}$ and SEC. A pseudo-linear first-order kinetic was observed for the monomer consumption over time, while in SEC elution traces, two distributions were observed (Figure 3B).

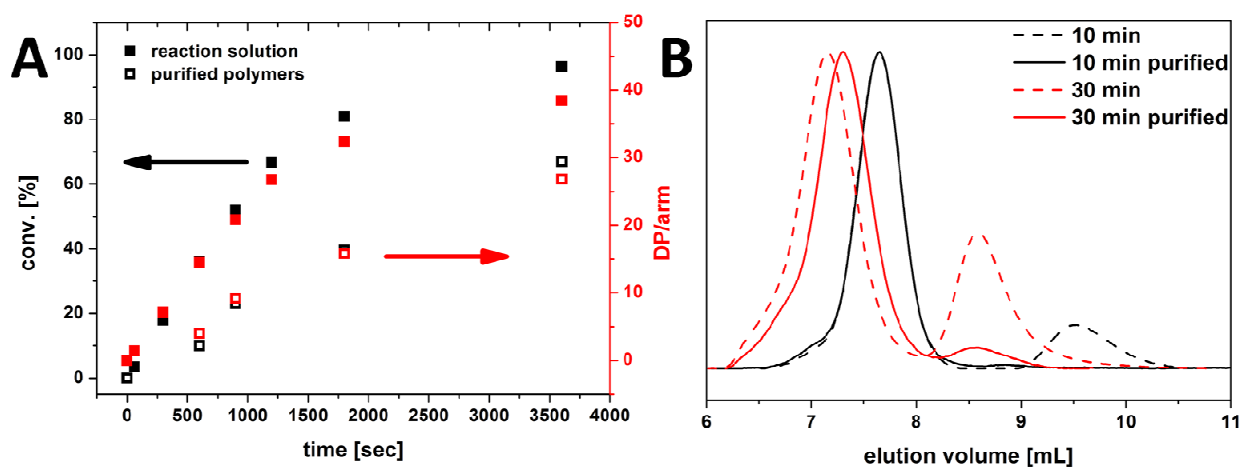
Taking into account the slope of the fit in Figure 3A, a propagation rate (k_p) of $337\text{ L mol}^{-1}\text{ s}^{-1} \times 10^{-3}$ can be calculated (corresponding to $42\text{ L mol}^{-1}\text{ s}^{-1} \times 10^{-3}$ per arm). However, as indicated by the second distribution in the SEC elution traces in Figure 3B, with increasing polymerization time, also homopolymer (PEtOx) is formed, presumably due to transfer reactions. Although $[\text{PEO}_{28}\text{-Ts}]_8$ has been extracted and co-evaporated with toluene several times prior to use, followed by drying for at least 24 h under vacuum, traces of impurities seem to persist.

Figure 3. First order time-conversion plot for the kinetic investigation of the microwave assisted polymerization of EtOx with [PEO₂₈-Ts]₈ as the initiator at 140 °C (A); comparison of the time-dependent SEC traces (CHCl₃) for the polymerization of EtOx (B).



One way to determine the actual amount of incorporated PEtOx within the star-shaped [PEO₂₈-*b*-PEtOx_x]₈ block copolymers is to remove the generated homopolymer via fractionated precipitation in THF at −30 °C. The results are depicted in Figure 4. Therefore, differences of up to 50% between the expected and the real PEtOx content can be observed. The monomer conversion obtained from the reaction solution seems to be up to 50% (DP = 20), but the monomer conversion determined via NMR from the purified product leads to 25% (DP = 10).

Figure 4. Time-dependent EtOx conversion (black squares) and the corresponding degrees of polymerization per arm (red squares) determined from the reaction mixture (filled squares) and after purification of the star-shaped block copolymers (empty squares) via NMR (A); SEC traces before (dashed line) and after purification via fractionated precipitation (B) (solid lines; CHCl₃ was used as the eluent).

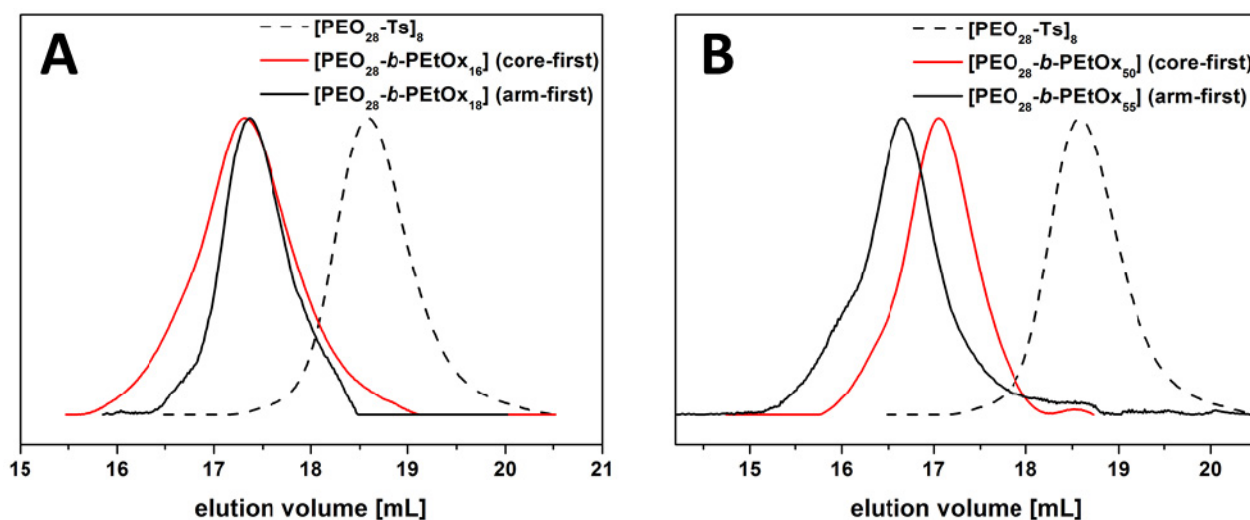


As can be seen in Figure 3B, after a polymerization time of 15 min, a considerable and clear shift of the desired product is visible in the elution traces and, at the same time, the amount of homopolymer formed is mediocre. The overall monomer conversion is around 50%, and we chose this as the conditions for the synthesis of samples with different PEtOx block lengths. Due to the fact that not

many differences were observed between $[\text{PEO}_{28}\text{-}b\text{-PEtOx}_{55}]_8$ and $[\text{PEO}_{28}\text{-}b\text{-PEtOx}_{75}]_8$ (Table 2), according to SEC measurements, $[\text{PEO}_{28}\text{-}b\text{-PEtOx}_{20}]_8$ and $[\text{PEO}_{28}\text{-}b\text{-PEtOx}_{60}]_8$ were targeted using the “core-first” approach, and the corresponding polymerizations were stopped at around 50% monomer conversion. The results are summarized in Table 2. In the case of the purified $[\text{PEO}_{28}\text{-}b\text{-PEtOx}_{50}]_8$, static light scattering (SLS) in THF was used in addition for the determination of the absolute molar mass (M_w). While in theory, a molar mass of $50,000 \text{ g mol}^{-1}$ would be expected for $[\text{PEO}_{28}\text{-}b\text{-PEtOx}_{50}]_8$ by the $[M]/[I]$ -ratio and NMR, SLS leads to a value of $54,000 \text{ g mol}^{-1}$, being in quite good agreement (Table 2).

We also compared the elution volume of star-shaped block copolymers with similar composition, but synthesized via two different approaches (Figure 5). As can be seen, for systems with a similar DP of roughly 20, the elution behavior is comparable via SEC (Figure 5A), as in NMR, the DP for the “arm-first” approach was 16, compared to 18 in the case of the “core-first” sample. For the star block copolymer with a higher amount of PEtOx (DP of 50), a shift to lower elution volume for the “core-first” product can be seen. Here, actual degrees of polymerization of 55 (“arm-first”) and 50 (“core-first”) for PEtOx were determined.

Figure 5. Comparison of the SEC traces obtained via the “core-first” (solid red lines) and the “arm-first” approach (solid black lines) in comparison to $[\text{PEO}_{28}\text{-Ts}]_8$ (dashed line) for two compositions: (A) $[\text{PEO}_{28}\text{-}b\text{-PEtOx}_{16}]_8$ (core-first; red curve) and $[\text{PEO}_{28}\text{-}b\text{-PEtOx}_{18}]_8$ (arm-first; black curve); and (B) $[\text{PEO}_{28}\text{-}b\text{-PEtOx}_{50}]_8$ (core-first; red curve) and $[\text{PEO}_{28}\text{-}b\text{-PEtOx}_{55}]_8$ (arm-first; black curve).



3.3. Study of Star-Shaped $[\text{PEO}_{28}\text{-}b\text{-PEtOx}_x]_8$ in Non-Selective Solvents

We were now interested in the solution properties of star-shaped $[\text{PEO}_{28}\text{-}b\text{-PEtOx}_x]_8$ block copolymers in non-selective solvents, for example, tetrahydrofuran (THF) or water. First, the hydrodynamic radii in solution were determined using dynamic light scattering (DLS). Therefore, the samples were dissolved in THF, filtered ($0.45 \mu\text{m}$, PTFE) and the size was compared to the crude $[\text{PEO}_{28}\text{-OH}]_8$ star polymer (Figure 6). According to the CONTIN plots depicted in Figure 6A, for $[\text{PEO}_{28}\text{-OH}]_8$, an apparent hydrodynamic radius of $\langle R_h \rangle_{n,\text{app}} = 1.5 \text{ nm}$ was observed, whereas for the

star-shaped block copolymers prepared via the “arm-first” approach, apparent hydrodynamic radii of 2.5 ([PEO₂₈-*b*-PEtOx₁₈]₈), 4 nm ([PEO₂₈-*b*-PEtOx₅₅]₈) and 5 nm ([PEO₂₈-*b*-PEtOx₇₅]₈) were determined under these conditions (Table 3). These results, in our opinion, both confirm the formation of unimers in THF and the elution behavior observed in SEC with increasing length of the outer PEtOx block. The hydrodynamic radii obtained for “core-first” [PEO₂₈-*b*-PEtOx₁₆]₈ (3 nm) and [PEO₂₈-*b*-PEtOx₅₀]₈ (3 nm) are comparable.

Figure 6. DLS CONTIN plot for “arm-first” approach stars in different solvents: in THF: [PEO₂₈-OH]₈ (dashed black line, $\langle R_h \rangle_{n,app} = 1.5$ nm), [PEO₂₈-*b*-PEtOx₁₈]₈ (red line, $\langle R_h \rangle_{n,app} = 2.5$ nm), [PEO₂₈-*b*-PEtOx₅₅]₈ (green line, $\langle R_h \rangle_{n,app} = 4$ nm) and [PEO₂₈-*b*-PEtOx₇₅]₈ (blue line, $\langle R_h \rangle_{n,app} = 5$ nm) (2 g L⁻¹) (A); in water [PEO₂₈-OH]₈ (dotted black line, $\langle R_h \rangle_{n,app} = 3$ nm), [PEO₂₈-*b*-PEtOx₁₈]₈ (red dashed, $\langle R_h \rangle_{n,app} = 6$ nm) and [PEO₂₈-*b*-PEtOx₇₅]₈ (blue line, $\langle R_h \rangle_{n,app} = 14$ nm) (0.5 g L⁻¹, filtered) (B).

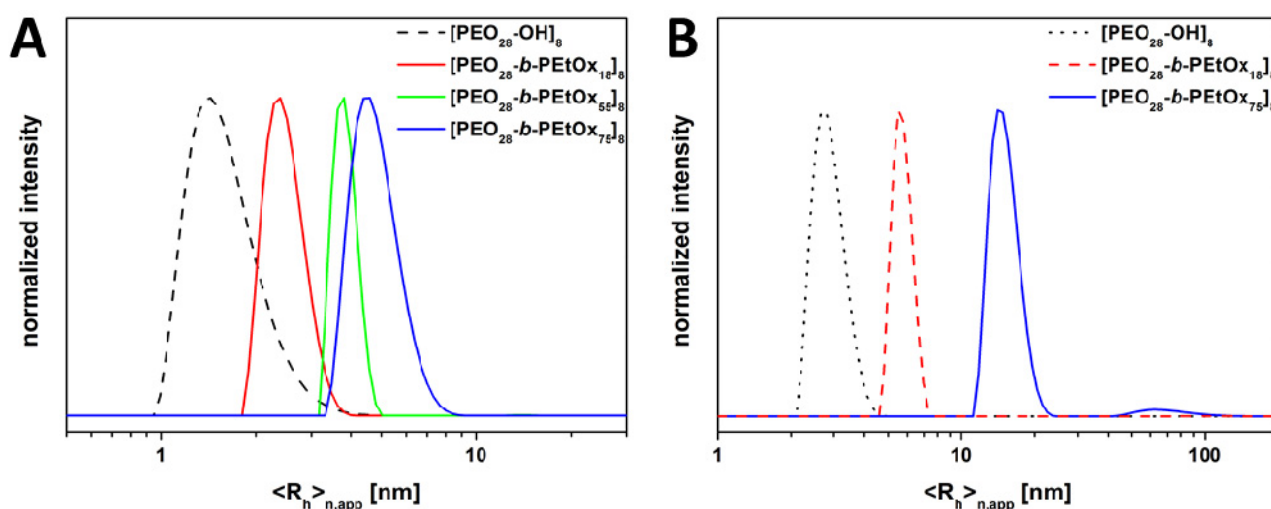


Table 3. Determination of the apparent hydrodynamic radius ($\langle R_h \rangle_{n,app}$) for different star (block co-) polymer systems in non-selective solvents via DLS.

Sample	approach	$\langle R_h \rangle_{n,app}$ ^a [nm] in THF	$\langle R_h \rangle_{n,app}$ ^a [nm] in H ₂ O
[PEO ₂₈ -OH] ₈	—	1.5	3
[PEO ₂₈ - <i>b</i> -PEtOx ₁₈] ₈	arm	2.5	6
[PEO ₂₈ - <i>b</i> -PEtOx ₁₆] ₈	core	3	3
[PEO ₂₈ - <i>b</i> -PEtOx ₅₅] ₈	arm	4	9
[PEO ₂₈ - <i>b</i> -PEtOx ₅₀] ₈	core	3	3
[PEO ₂₈ - <i>b</i> -PEtOx ₇₅] ₈	arm	5	14/62
[PEO ₂₈ - <i>b</i> -PEtOx ₁₈] ₈ ^c	arm	—	92/283 ^b
[PEO ₂₈ - <i>b</i> -PEtOx ₇₅] ₈ ^c	arm	—	72 ^b

^a determined via CONTIN plot; ^b CONTIN plots in the Supporting Information part Figure S7; ^c non filtered sample.

However, if these “arm-first” materials are directly dissolved in water, again, a non-selective solvent for both PEO and PEtOx, turbid solutions are obtained. Transferring the materials from THF to water, via dialysis or evaporation of the organic co-solvent, leads to the same result. The turbidity did

not decrease after heating (up to 100 °C), cooling (~5 °C for one week), changing the pH (0 to 12), prolonged sonication or the addition of different salts (e.g., KSCN, NaCl, KCl). For these turbid solutions, hydrodynamic radii of up to several hundred nm were observed, even at very low concentrations ($<0.5 \text{ g L}^{-1}$, Table 3, Figure S8). At this point, we assume that this turbidity originates from the aggregation of the star-shaped block copolymers, although both blocks are of hydrophilic nature. Such behavior has also been described for water-soluble homo- and block copolymers in the literature [12,19,56–58]. In some cases, the unexpected aggregation of double-hydrophilic block copolymers was explained by slight differences in the hydrophilicity of both blocks [50,58].

If, on the other hand, star-shaped $[\text{PEO}_{28}\text{-}b\text{-PEtOx}_x]_8$ block copolymers synthesized via the “core-first” approach were treated the same way, clear aqueous solutions with hydrodynamic radii of ~3 nm (both cases) are obtained. Somehow, the effect of aggregation in aqueous media is limited to samples prepared by click chemistry, for which we have no conclusive explanation up to now. No detectable amounts of copper were found in atom absorption spectroscopy (AAS), and therefore, an influence of residual copper from the CuAAC reaction can be excluded.

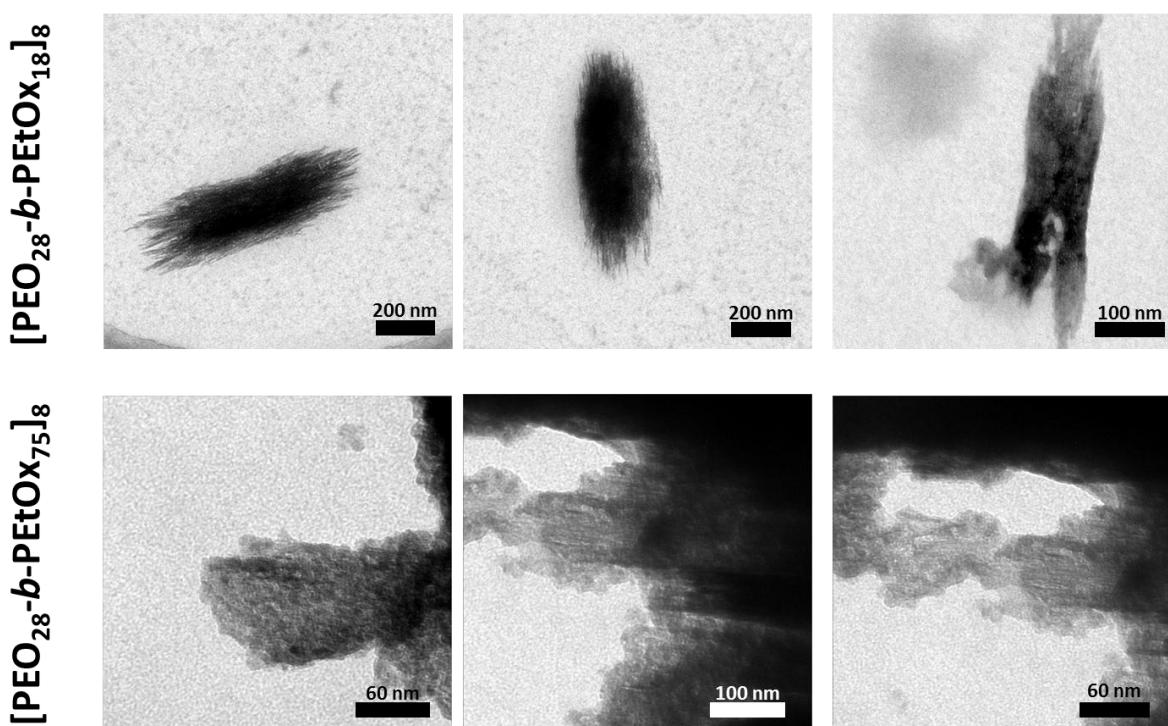
Applying shear forces via filtration (syringe filter, 1 μm , GF) to the turbid solutions of all described “arm-first” samples leads to clear solutions. To ensure that no material was removed by filtration, a defined concentration was filtered and dried afterwards, and the weight loss was below 5%. In Figure 6B, the DLS CONTIN plots for $[\text{PEO}_{28}\text{-OH}]_8$ (dashed black line, $\langle R_h \rangle_{n,\text{app}} = 3 \text{ nm}$), $[\text{PEO}_{28}\text{-}b\text{-PEtOx}_{18}]_8$ (red line, $\langle R_h \rangle_{n,\text{app}} = 6 \text{ nm}$) and $[\text{PEO}_{28}\text{-}b\text{-PEtOx}_{75}]_8$ (blue line, $\langle R_h \rangle_{n,\text{app}} = 14 \text{ nm}$) are depicted. The obtained size distributions by DLS are slightly larger if compared to THF ($\langle R_h \rangle_{n,\text{app}} = 1.5 \text{ nm}$, 2.5 nm and 5 nm), respectively. This might be an indication for the formation of aggregates by entanglements or that the star-shaped block copolymers are highly swollen.

It is well known that PEtOx materials exhibit lower critical solution temperatures (LCST), depending on the chain length [47,59]. To probe this for the herein described star-shaped systems, solutions of $[\text{PEO}_{28}\text{-}b\text{-PEtOx}_{20}]_8$ and $[\text{PEO}_{28}\text{-}b\text{-PEtOx}_{80}]_8$ (2.5 mg mL^{-1} , non-filtered aqueous solution) were heated up to 100 °C, and the turbidity was recorded. In both cases, the solutions did not show cloud points. We ascribe the absence of LCST behavior to the presence of a double-hydrophilic system and, in the case of $[\text{PEO}_{28}\text{-}b\text{-PEtOx}_{20}]_8$, to the short PEtOx arms.

As another peculiarity, it has been reported by Demirel *et al.* that PEtOx with a molar mass of 500 kg mol^{-1} (1 mg mL^{-1}) crystallizes after being heated in dilute solutions for several days at 70 °C [60]. We therefore were interested in whether similar observations can be made for star-shaped systems of different composition. Solutions of $[\text{PEO}_{28}\text{-}b\text{-PEtOx}_{18}]_8$ and $[\text{PEO}_{28}\text{-}b\text{-PEtOx}_{75}]_8$ were heated to 80 °C in water for three days. No changes could be detected for the materials synthesized using the “core-first” approach, whereas larger aggregates were found by DLS and transmission electron microscopy (TEM) for $[\text{PEO}_{28}\text{-}b\text{-PEtOx}_{18}]_8$ and $[\text{PEO}_{28}\text{-}b\text{-PEtOx}_{80}]_8$ prepared via the “arm-first” methodology (Figure 7, only if unfiltered solutions were used). The structure of such aggregates was different, depending on whether $[\text{PEO}_{28}\text{-}b\text{-PEtOx}_{18}]_8$ (55 wt % PEtOx) or $[\text{PEO}_{28}\text{-}b\text{-PEtOx}_{75}]_8$ (82 wt % PEtOx) was used. In the case of $[\text{PEO}_{28}\text{-}b\text{-PEtOx}_{18}]_8$, sharp, crystal-like structures were observed, possibly due to partial crystallization of PEtOx, which was also observed by Güner *et al.*, [60] leading to an alignment in a rod-like fashion (Figure 7A). Assemblies of several hundred nm in length and ~200 nm width were obtained. For $[\text{PEO}_{28}\text{-}b\text{-PEtOx}_{75}]_8$, a slightly different aggregation mechanism might take place: here, the superstructures, rather, look like micellar clusters,

which might be the result of an initial formation of unimolecular micelles, followed by further agglomeration (Figure 7B) [61,62]. Tentatively, the hydrophilicity of PEtOx might be lower in comparison to PEO; we assume a partial collapse of the outer PEtOx shell over time, leading to aggregation. However, as this effect was only observed for star-shaped block copolymers prepared via the “arm first” approach and only if non-filtered solutions were used, we hypothesize that a certain pre-organization is required. The aggregation behavior of PEO depending on the treatment before was also discussed by Güner *et al.* for linear polymers [56], and differences in hydrophilicity were described by Ke *et al.* [50,60].

Figure 7. TEM micrographs of aggregates formed by $[\text{PEO}_{28}\text{-}b\text{-PEtOx}_{18}]_8$ (**top**) and $[\text{PEO}_{28}\text{-}b\text{-PEtOx}_{75}]_8$ (**bottom**) after heating for three days at 80 °C (unfiltered solutions, “arm-first” approach).



4. Conclusions

We demonstrated the synthesis of a series of well-defined star-shaped $[\text{PEO}_{28}\text{-}b\text{-PEtOx}_x]_8$ block copolymers using two different approaches, either “core-first” using $[\text{PEO}_{28}\text{-Ts}]_8$ as a macroinitiator for the CROP of EtOx or by copper-catalyzed azide-alkyne cycloadditions between $[\text{PEO}_{28}\text{-N}_3]_8$ and TB-PEtOx_x (“arm-first”). In both cases, different block lengths for the outer PEtOx block were used, and comparable molar masses and hydrodynamic radii in THF as a non-selective solvent were observed. In dilute aqueous solutions, samples prepared via the “arm-first” approach showed aggregate formation, whereas this was not the case for the “core-first” materials. Although this behavior is not fully understood at this point, we could exclude several factors (salt, copper impurities, differences in the molar mass) as the origin of this peculiarity, and we could show that after filtration (1 μm pore size), also, here, smaller hydrodynamic radii are found. At this point, our hypothesis is that small differences in hydrophilicity are the main driving force for this behavior. More importantly, such loose

aggregates from star-shaped block copolymers could be used for the temperature-induced formation of larger agglomerates, where first investigations hint towards an influence of the weight ratio PEO:PEtOx on the morphology of the superstructures formed.

Acknowledgments

We thank Grit Festag for help with the SEC analysis, Sandra Köhn for AAS measurements, Nicole Fritz for help with the 2D-LC and Frank Steiniger and Christine Kämnitz (Electron Microscope Center Jena) for help with the TEM. F.H.S. and T.R. are further grateful to the Thuringian Ministry for Education, Science and Culture (TMBWK; #B515-10065, ChaPoNano) for financial support. F.H.S. thanks the VCI for a starting an independent researcher fellowship, and T.R. acknowledges the Carl-Zeiss foundation for a PhD-scholarship. We also wish to acknowledge the Dutch Polymer Institute (DPI, technology area high-throughput-experimentation, project #690) and the Thuringian Ministry for Education, Science and Culture (grants #B514-09051, NanoConSens, #B515-11028, SWAXS-JCSM and #03WKCB01C, BASIS and #B515-07008) for financial support of this study.

Conflicts of Interest

The authors declare no conflict of interest.

References

1. Barner-Kowollik, C.; Lutz, J.-F.; Perrier, S. New methods of polymer synthesis. *Polym. Chem.* **2012**, *3*, 1677–1679.
2. Pitsikalis, M.; Pispas, S.; Mays, J.W.; Hadjichristidis, N. Nonlinear Block Copolymer Architectures. In *Blockcopolymers–Polyelectrolytes–Biodegradation*; Advances in Polymer Science; Springer-Verlag: Berlin/Heidelberg, Germany, 1998; Volume 135, pp. 1–137.
3. Burchard, W. Solution Properties of Branched Macromolecules. *Adv. Polym. Sci.* **1999**, *143*, 113–194.
4. Hadjichristidis, N.; Pispas, S.; Pitsikalis, M.; Iatrou, H.; Vlahos, C. Asymmetric Star Polymers: Synthesis and Properties; In *Branched Polymers I*; Advances in Polymer Science; Roovers, J., Ed.; Springer: Berlin/Heidelberg, Germany, 1999; Volume 142, pp. 71–127.
5. Plamper, F.A.; McKee, J.R.; Laukkanen, A.; Nykanen, A.; Walther, A.; Ruokolainen, J.; Aseyev, V.; Tenhu, H. Miktoarm stars of poly(ethylene oxide) and poly(dimethylaminoethyl methacrylate): manipulation of micellization by temperature and light. *Soft Matter* **2009**, *5*, 1812–1821.
6. Hadjichristidis, N.; Pitsikalis, M.; Pispas, S.; Iatrou, H. Polymers with Complex Architecture by Living Anionic Polymerization. *Chem. Rev.* **2001**, *101*, 3747–3792.
7. Matyjaszewski, K.; Xia, J.H. Atom transfer radical polymerization. *Chem. Rev.* **2001**, *101*, 2921–2990.
8. Moad, G.; Rizzardo, E.; Thang, S.H. Living radical polymerization by the RAFT process. *Aust. J. Chem.* **2005**, *58*, 379–410.

9. Schacher, F.H.; Rupa, P.A.; Manners, I. Functional Block Copolymers: Nanostructured Materials with Emerging Applications. *Angew. Chem. Int. Ed.* **2012**, *51*, 7898–7921.
10. Zhang, J.; Lu, Z.-Y.; Sun, Z.-Y. Self-assembly structures of amphiphilic multiblock copolymer in dilute solution. *Soft Matter* **2013**, *9*, 1947–1954.
11. Gröschel, A.H.; Schacher, F.H.; Schmalz, H.; Borisov, O.V.; Zhulina, E.B.; Walther, A.; Müller, A.H.E. Precise hierarchical self-assembly of multicompartment micelles. *Nat. Commun.* **2012**, *3*, 710.
12. Riess, G. Micellization of block copolymers. *Prog. Polym. Sci.* **2003**, *28*, 1107–1170.
13. Schacher, F.; Walther, A.; Müller, A.H.E. Dynamic Multicompartment-Core Micelles in Aqueous Media. *Langmuir* **2009**, *25*, 10962–10969.
14. Förster, S.; Abetz, V.; Müller, A.H.E. *Polyelectrolyte Block Copolymer Micelles*; Springer Berlin: Heidelberg, Germany, 2004.
15. Iatridi, Z.; Tsitsilianis, C. Water-Soluble Stimuli Responsive Star-Shaped Segmented Macromolecules. *Polymers* **2011**, *3*, 1911–1933.
16. Schacher, F.H.; Elbert, J.; Patra, S.K.; Mohd Yusoff, S.F.; Winnik, M.A.; Manners, I. Responsive Vesicles from the Self-Assembly of Crystalline-Coil Polyferrocenylsilane-*block*-Poly(ethylene Oxide) Star-Block Copolymers. *Chem. Eur. J.* **2012**, *18*, 517–525.
17. Schacher, F.H.; Freier, U.; Steiniger, F. Hierarchical self-assembly of star-shaped organometallic crystalline-coil block copolymers in solution. *Soft Matter* **2012**, *8*, 6968–6978.
18. Steinschulte, A.A.; Schulte, B.; Erberich, M.; Borisov, O.V.; Plamper, F.A. Unimolecular Janus Micelles by Microenvironment-Induced, Internal Complexation. *ACS Macro Lett.* **2012**, *1*, 504–507.
19. Knop, K.; Pavlov, G.M.; Rudolph, T.; Martin, K.; Pretzel, D.; Jahn, B.O.; Scharf, D.H.; Brakhage, A.A.; Makarov, V.; Mollmann, U.; Schacher, F.H.; Schubert, U.S. Amphiphilic star-shaped block copolymers as unimolecular drug delivery systems: investigations using a novel fungicide. *Soft Matter* **2013**, *9*, 715–726.
20. Lapienis, G. Star-shaped polymers having PEO arms. *Prog. Polym. Sci.* **2009**, *34*, 852–892.
21. Quaglia, F.; Ostacolo, L.; Nese, G.; Canciello, M.; de Rosa, G.; Ungaro, F.; Palumbo, R.; la Rotonda, M.I.; Maglio, G. Micelles based on amphiphilic PCL-PEO triblock and star-shaped diblock copolymers: Potential in drug delivery applications. *J. Biomed. Mater. Res. A* **2008**, *87A*, 563–574.
22. Knop, K.; Hoogenboom, R.; Fischer, D.; Schubert, U.S. Poly(ethylene glycol) in Drug Delivery: Pros and Cons as Well as Potential Alternatives. *Angew. Chem. Int. Ed.* **2010**, *49*, 6288–6308.
23. Hanisch, A.; Schmalz, H.; Müller, A.H.E. A Modular Route for the Synthesis of ABC Miktoarm Star Terpolymers via a New Alkyne-Substituted Diphenylethylene Derivative. *Macromolecules* **2012**, *45*, 8300–8309.
24. Altintas, O.; Vogt, A.P.; Barner-Kowollik, C.; Tunca, U. Constructing star polymers via modular ligation strategies. *Polym. Chem.* **2012**, *3*, 34–45.
25. Fijten, M.W.M.; Haensch, C.; van Lankvelt, B.M.; Hoogenboom, R.; Schubert, U.S. Clickable poly(2-oxazoline)s as versatile building blocks. *Macromol. Chem. Phys.* **2008**, *209*, 1887–1895.

26. Hadjichristidis, N.; Iatrou, H.; Pitsikalis, M.; Pispas, S.; Avgeropoulos, A. Linear and non-linear triblock terpolymers. Synthesis, self-assembly in selective solvents and in bulk. *Prog. Polym. Sci.* **2005**, *30*, 725–782.
27. Kempe, K.; Krieg, A.; Becer, C.R.; Schubert, U.S. “Clicking” on/with polymers: A rapidly expanding field for the straightforward preparation of novel macromolecular architectures. *Chem. Soc. Rev.* **2012**, *41*, 176–191.
28. Tsitsilianis, C.; Lutz, P.; Graff, S.; Lamps, J.P.; Rempp, P. Core-first synthesis of star polymers with potentially ionogenic branches. *Macromolecules* **1991**, *24*, 5897–5902.
29. Knischka, R.; Lutz, P.J.; Sunder, A.; Mülhaupt, R.; Frey, H. Functional Poly(ethylene oxide) Multiarm Star Polymers: Core-First Synthesis Using Hyperbranched Polyglycerol Initiators. *Macromolecules* **2000**, *33*, 315–320.
30. Schmidt, B.V.K.J.; Rudolph, T.; Hetzer, M.; Ritter, H.; Schacher, F.H.; Barner-Kowollik, C. Supramolecular three-armed star polymers via cyclodextrin host-guest self-assembly. *Polym. Chem.* **2012**, *3*, 3139–3145.
31. Altintas, O.; Tunca, U.; Barner-Kowollik, C. Star and miktoarm star block (co)polymers via self-assembly of ATRP generated polymer segments featuring Hamilton wedge and cyanuric acid. *Polym. Chem.* **2011**, *2*, 1146–1155.
32. Hochwimmer, G.; Nuyken, O.; Schubert, U.S. 6,6'-Bisfunctionalized 2,2'-bipyridines as metallo-supramolecular initiators for the living polymerization of oxazolines. *Macromol. Rapid Comm.* **1998**, *19*, 309–313.
33. Altintas, O.; Yankul, B.; Hizal, G.; Tunca, U. One-pot preparation of 3-miktoarm star terpolymers via click [3 + 2] reaction. *J. Polym. Sci. A Polym. Chem.* **2007**, *45*, 3588–3598.
34. Johnson, J.A.; Finn, M.G.; Koberstein, J.T.; Turro, N.J. Construction of Linear Polymers, Dendrimers, Networks, and Other Polymeric Architectures by Copper-Catalyzed Azide-Alkyne Cycloaddition “Click” Chemistry. *Macromol. Rapid Comm.* **2008**, *29*, 1052–1072.
35. Chen, C.H.; Wilson, J.; Chen, W.; Davis, R.M.; Riffle, J.S. A light-scattering study of poly(2-alkyl-2-oxazoline)s: effect of temperature and solvent type. *Polymer* **1994**, *35*, 3587–3591.
36. Carmichael, A.Y.; Caba, B.L.; Huffstetler, P.P.; Davis, R.M.; Riffle, J.S. Synthesis and solution properties of poly(ethylene oxide-*b*-2-ethyl-2-oxazoline) and poly(ethylene oxide-*b*-ethyleneimine). *Polym. Prepr.* **2004**, *45*, 476–477.
37. Schlaad, H.; Diehl, C.; Gress, A.; Meyer, M.; Demirel, A.L.; Nur, Y.; Bertin, A. Poly(2-oxazoline)s as Smart Bioinspired Polymers. *Macromol. Rapid Commun.* **2010**, *31*, 511–525.
38. Park, J.-S.; Kataoka, K. Comprehensive and Accurate Control of Thermosensitivity of Poly(2-alkyl-2-oxazoline)s via Well-Defined Gradient or Random Copolymerization. *Macromolecules* **2007**, *40*, 3599–3609.
39. Bauer, M.; Lautenschlaeger, C.; Kempe, K.; Tauhardt, L.; Schubert, U.S.; Fischer, D. Poly(2-ethyl-2-oxazoline) as Alternative for the Stealth Polymer Poly(ethylene glycol): Comparison of in vitro Cytotoxicity and Hemocompatibility. *Macromol. Biosci.* **2012**, *12*, 986–998.

40. Rudolph, T.; Kempe, K.; Crotty, S.; Paulus, R.M.; Schubert, U.S.; Krossing, I.; Schacher, F.H. A strong cationic Bronsted acid, $[H(OEt_2)_2][Al\{OC(CF_3)_3\}_4]$, as an efficient initiator for the cationic ring-opening polymerization of 2-alkyl-2-oxazolines. *Polym. Chem.* **2013**, *4*, 495–505.
41. Tauhardt, L.; Kempe, K.; Knop, K.; Altuntaş, E.; Jäger, M.; Schubert, S.; Fischer, D.; Schubert, U.S. Linear Polyethyleneimine: Optimized Synthesis and Characterization—On the Way to “Pharmagrade” Batches. *Macromol. Chem. Phys.* **2011**, *212*, 1918–1924.
42. Einzmann, M.; Binder, W.H. Novel functional initiators for oxazoline polymerization. *J. Polym. Sci. A Polym. Chem.* **2001**, *39*, 2821–2831.
43. Kobayashi, S.; Uyama, H.; Narita, Y.; Ishiyama, J. Novel multifunctional initiators for polymerization of 2-oxazolines. *Macromolecules* **1992**, *25*, 3232–3236.
44. Knop, K.; Jahn, B.O.; Hager, M.D.; Crecelius, A.; Gottschaldt, M.; Schubert, U.S. Systematic MALDI-TOF CID Investigation on Different Substituted mPEG 2000. *Macromol. Chem. Phys.* **2010**, *211*, 677–684.
45. Li, Z.; Chau, Y. A facile synthesis of branched poly(ethylene glycol) and its heterobifunctional derivatives. *Polym. Chem.* **2011**, *2*, 873–878.
46. Güner, P. T.; Demirel, A.L. Effect of Anions on the Cloud Point Temperature of Aqueous Poly(2-ethyl-2-oxazoline) Solutions. *J. Phys. Chem. B* **2012**, *116*, 14510–14514.
47. Christova, D.; Velichkova, R.; Loos, W.; Goethals, E.J.; Prez, F.D. New thermo-responsive polymer materials based on poly(2-ethyl-2-oxazoline) segments. *Polymer* **2003**, *44*, 2255–2261.
48. Kolb, H.C.; Finn, M.G.; Sharpless, K.B. Click Chemistry: Diverse Chemical Function from a Few Good Reactions. *Angew. Chem. Int. Ed.* **2001**, *40*, 2004–2021.
49. Rostovtsev, V.V.; Green, L.G.; Fokin, V.V.; Sharpless, K.B. A Stepwise Huisgen Cycloaddition Process: Copper(I)-Catalyzed Regioselective “Ligation” of Azides and Terminal Alkynes. *Angew. Chem. Int. Ed.* **2002**, *114*, 2708–2711.
50. Ke, F.; Mo, X.; Yang, R.; Wang, Y.; Liang, D. Association of Block Copolymer in Nonselective Solvent. *Macromolecules* **2009**, *42*, 5339–5344.
51. Malik, M.I.; Ahmed, H.; Trathnigg, B. Liquid chromatography under critical conditions: practical applications in the analysis of amphiphilic polymers. *Anal. Bioanal. Chem.* **2009**, *393*, 1797–1804.
52. Falkenhagen, J.; Much, H.; Stauf, W.; Müller, A.H.E. Characterization of Block Copolymers by Liquid Adsorption Chromatography at Critical Conditions. 1. Diblock Copolymers. *Macromolecules* **2000**, *33*, 3687–3693.
53. Jiang, W.; Khan, S.; Wang, Y. Retention Behaviors of Block Copolymers in Liquid Chromatography at the Critical Condition. *Macromolecules* **2005**, *38*, 7514–7520.
54. Sharghi, H.; Khalifeh, R.; Doroodmand, M.M. Immobilization of Porphyrinatocopper Nanoparticles onto Activated Multi-Walled Carbon Nanotubes and a Study of its Catalytic Activity as an Efficient Heterogeneous Catalyst for a Click Approach to the Three-Component Synthesis of 1,2,3-Triazoles in Water. *Adv. Synth. Catal.* **2009**, *351*, 207–218.
55. Ziegast, G.; Pfannemüller, B. Linear and star-shaped hybrid polymers, 1. A new method for the conversion of hydroxyl end groups of poly(oxyethylene) and other polyols into amino end groups. *Makromol. Chem.* **1984**, *5*, 363–371.

56. Özdemir, C.; Güner, A. Solubility profiles of poly(ethylene glycol)/solvent systems, I: Qualitative comparison of solubility parameter approaches. *Eur. Polym. J.* **2007**, *43*, 3068–3093.
57. Nakashima, K.; Bahadur, P. Aggregation of water-soluble block copolymers in aqueous solutions: Recent trends. *Adv. Col. Int. Sci.* **2006**, *123–126*, 75–96.
58. Casse, O.; Shkilnyy, A.; Linders, J.; Mayer, C.; Häussinger, D.; Völkel, A.; Thünemann, A.F.; Dimova, R.; Cölfen, H.; Meier, W.; Schlaad, H.; Taubert, A. Solution Behavior of Double-Hydrophilic Block Copolymers in Dilute Aqueous Solution. *Macromolecules* **2012**, *45*, 4772–4777.
59. Lambermont-Thijs, H.M.L.; Kuringen, H.P.C.V.; Put, J.P.W.V.D.; Schubert, U.S.; Hoogenboom, R. Temperature Induced Solubility Transitions of Various Poly(2-oxazoline)s in Ethanol-Water Solvent Mixtures. *Polymers* **2010**, *2*, 188–199.
60. Guner, P.T.; Miko, A.; Schweinberger, F.F.; Demirel, A.L. Self-assembled poly(2-ethyl-2-oxazoline) fibers in aqueous solutions. *Polym. Chem.* **2012**, *3*, 322–324.
61. Cheng, L.; Zhang, G.; Zhu, L.; Chen, D.; Jiang, M. Nanoscale tubular and sheetlike superstructures from hierarchical self-assembly of polymeric janus particles. *Angew. Chem. Int. Ed.* **2008**, *47*, 10171–10174.
62. Liu, C.; Zhang, K.; Chen, D.; Jiang, M.; Liu, S. Transforming spherical block polyelectrolyte micelles into free-suspending films via DNA complexation-induced structural anisotropy. *Chem. Commun.* **2010**, *46*, 6135–6137.